Epitaxy of Ge–Sb–Te phase-change memory alloys

Wolfgang Braun,[1,a)] Roman Shayduk,[1] Timur Flissikowski,[1] Manfred Ramsteiner,[1] Holger T. Grahn,[1] Henning Riechert,[1] Paul Fons,[2] and Alex Kolobov[2]
[1]*Paul Drude Institute for Solid State Electronics, Hausvogteiplatz 5-7, 10117 Berlin, Germany*
[2]*Center for Applied Near-Field Optics Research, National Institute of Advanced Industrial Science and Technology, Tsukuba Central 4, 1-1-1 Higashi, Tsukuba, Ibaraki 305-8562, Japan*

(Received 2 October 2008; accepted 28 December 2008; published online 26 January 2009)

The authors demonstrate the epitaxy of Ge–Sb–Te alloys close to the $Ge_2Sb_2Te_5$ composition on GaSb(001). Using molecular beam epitaxy with elemental sources, amorphous films are obtained at growth temperatures below 120 °C and films with a cubic structure and a predominant cube-on-cube epitaxial relationship above 180 °C. Using a high-power pulsed laser, the epitaxial films are switched between the crystalline and the amorphous phases. Streaks in the diffraction data help to resolve the apparent ambiguity in interatomic distances between earlier x-ray absorption and powder diffraction measurements. The structural changes are confirmed by Raman spectroscopy. © *2009 American Institute of Physics*. [DOI: 10.1063/1.3072615]

Phase-change materials as exemplified by quasibinary alloys in the $GeTe-Sb_2Te_3$ (GST) system, specifically $Ge_2Sb_2Te_5$, are at the heart of a variety of *nonvolatile* memory devices such as rewritable digital versatile disks commercialized by Matsushita in the 1990s and electrical phase-change random access memory (PCRAM), which is under active development. Recently, interest in PCRAM has intensified since it possesses much better scalability and speed than the currently used Flash memory and is likely to replace the latter in the coming years.[1]

The basic idea behind phase-change memory is quite simple: The structure is switched between the *metastable* crystalline and amorphous states by optical and/or electrical pulses of different intensity and duration. The details of the structural changes, however, are still a matter of controversy. The large electronic differences between the amorphous and crystalline phases have been ascribed to the presence of *resonant* bonding in the metastable crystalline state and its corresponding absence in the amorphous state. Part of the difficulty in obtaining a clearer understanding of the switching process is that the crystalline (amorphous) phase is metastable and can only be fabricated in thin polycrystalline (or amorphous) film form. The high temperatures required for single crystal growth lead to formation of the stable nine-layer rhombohedral phase. Crystalline GST has been suggested to assume the rocksalt structure with a rather large isotropic temperature factor based on Rietveld refinement of polycrystalline GST.[2] Extended x-ray absorption fine-structure (EXAFS) based examination of the structure of the crystalline phase, however, has demonstrated the presence of a Peierls-like splitting of nearest neighbor distances into shorter and longer bonds. The EXAFS determined shorter Ge–Te (2.83 Å) bond lengths that are significantly smaller than that expected (3.02 Å) based on the powder diffraction determined unit cell.[3]

These results, although shedding significant light on the phase-change mechanism, intrinsically lack completeness. X-ray diffraction on the one hand measures an ensemble average and when applied to a polycrystal is not able to distinguish between Ge atoms being statically or dynamically displaced from the center, i.e., whether Ge atoms are indeed very loose and mobile within the lattice or stochastically displaced from their ideal high symmetry positions. EXAFS, on the other hand, is a local (and very fast) probe and can unambiguously identify local displacements. It is difficult, however, to unambiguously determine the direction of the displacement from EXAFS alone. The present consensus is that GST possesses a distorted rocksalt structure, but further details are missing. Since correlated distortions may be a key issue to understand certain aspects of the recording process, it is crucial to grow and investigate single crystal samples. According to powder diffraction data,[2] the cubic phase of $Ge_2Sb_2Te_5$ has a lattice constant of 6.02 Å. It should therefore match GaSb with a misfit of 1.3%.

In this work, we investigate the epitaxial growth of GST close to the $Ge_2Sb_2Te_5$ composition on GaSb(001). The experiments were carried out in our combined molecular beam epitaxy (MBE) chamber and diffractometer[4] at the synchrotron BESSY in Berlin at a chamber pressure around 1×10^{-9} mbar. The solid source effusion cell temperatures were 1092, 536, and 346 °C during deposition for Ge, Sb, and Te, respectively, resulting in a GST growth rate of 0.4 nm/min. 1 mm thick GaSb(001) substrates with a misorientation of less than 0.02° were used. The native oxide was thermally desorbed and a 50 nm thick buffer was grown using established III/V growth techniques.[5,6] The substrate temperature was controlled by a thermocouple, the reported[5,6] oxide desorption temperature of 530 °C served as a reference point. The growth process was monitored *in situ* by reflection high-energy electron diffraction (RHEED) and surface x-ray diffraction under ultrahigh vacuum conditions.

Figure 1 shows nine RHEED screenshots recorded every 20 s during growth of a typical sample at a substrate temperature of 200 °C. Deposition starts from the GaSb (1×5) reconstruction. The first stage of the growth is characterized by the formation of an approximately 0.6 nm thick amorphous layer. We observe decreasing intensities of the RHEED reflections until they completely vanish at about 100 s in the growth. Subsequently, epitaxial material inherit-

a)Electronic mail: braun@pdi-berlin.de. URL: www.pdi-berlin.de.

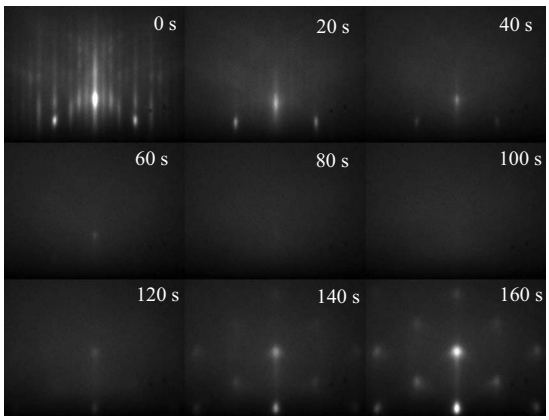

FIG. 1. RHEED diffraction patterns recorded every 20 s during GST growth. The epitaxial film nucleates from an amorphous intermediate layer.

ing the cubic symmetry of the substrate nucleates out of this film. The appearance of a transmission pattern at 120 s implies a fairly rough surface, which is consistent with scanning electron microscopy images of thicker layers (not shown) revealing several nanometer high crystallites bounded predominantly by (111) facets, but abrupt and stable interfaces with the substrate. Since cubic GST probably contains about 20% vacancies on the Ge/Sb sublattice,[2] we speculate that crystallization initially takes place inside the amorphous layer, where the formation of these voids may be easier than at the surface. The grains having an orientation close to the ideal epitaxial relationship then experience an energy gain due to their reduced interface energy with the substrate and grow faster than differently oriented ones. Further growth continues three dimensionally, with a sharpening and strengthening of the transmission spots.

The out-of-plane cuts through reciprocal space obtained from the RHEED patterns shown in Figs. 2(a) and 2(b) along the [110] and [100] axes indicate full three-dimensional epitaxy of the layer and a body-centered reciprocal lattice, therefore demonstrating that the average real space structure of the film is face-centered cubic. The in-plane azimuthal scan shown in Fig. 2(c) (see Ref. 7 for a description of this method) confirms the in-plane epitaxy of the GST layer and the presence of a cubic crystal structure. Streaks extending

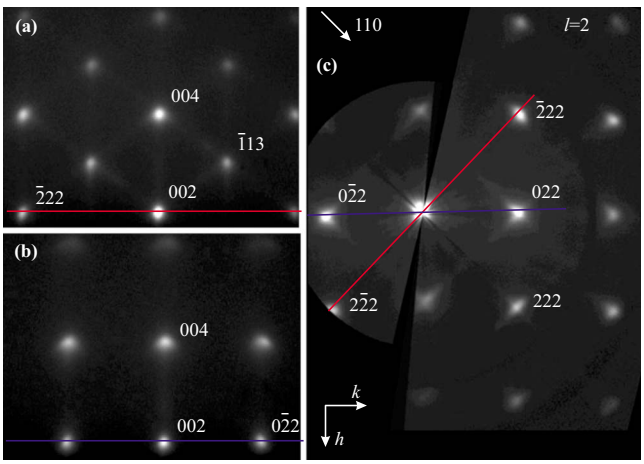

FIG. 2. (Color online) Two RHEED screenshots along (a) the [110] and (b) the [100] azimuth and (c) the corresponding azimuthal scan in the $l=2$ plane as indicated by the lines common to each pair. The nominal film thickness is 30 nm.

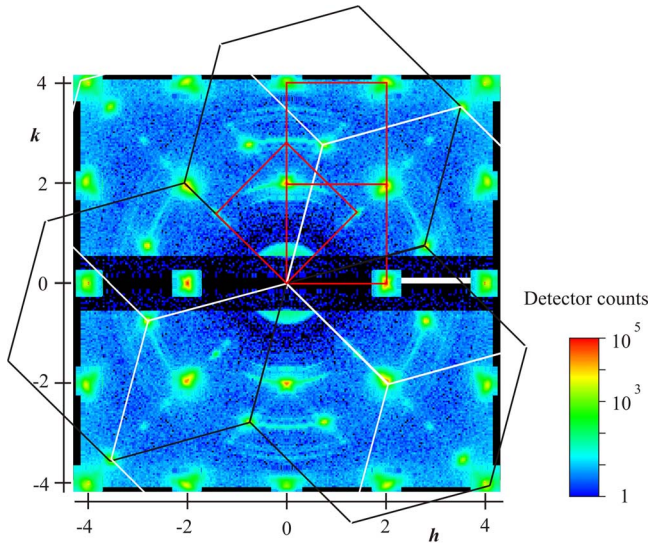

FIG. 3. (Color online) Reciprocal space plane parallel to the surface at $l=0.05$ obtained by x-ray diffraction. Lines indicate different in-plane symmetries present in the film.

from the reflections in plane along the ⟨110⟩ and out-of-plane along the ⟨111⟩ axes imply relaxation and facet formation along the ⟨111⟩ directions, indicating that the Peierls distortion observed by EXAFS is preferentially directed along ⟨111⟩. Out-of-plane x-ray measurements (not shown) are also consistent with this interpretation.

Figure 3 shows grazing incidence x-ray diffraction data from the same film in the reciprocal plane parallel to the surface at $l=0.05$, close to the origin of the reciprocal lattice. The color gradient represents the detector counts on a logarithmic scale. The film predominantly consists of two epitaxial orientations, with either the [001] or the [111] axis of the film parallel to the substrate (001) surface normal. The measured lattice constant of 6.01 Å is very close to literature values[8–10] for cubic GST fabricated by sputtering. The preferential orientation is cube on cube, with small amounts of 45° rotated domains (red squares). The circular segments in the scan indicate crystalline grains with various intermediate rotations. No hexagonal structure c-axis reflections are found normal to the surface (not shown), confirming the absence of hexagonal GST.

The relative elemental flux rates for the sample shown in Fig. 3 were 1.6:1.9:5 for Ge:Sb:Te, as determined from fluorescence spectra taken from amorphous films deposited on Si substrates at around 160 °C. Layers grown with compositions less than 2% off of 2:2:5 showed very similar diffraction intensities both in RHEED and in x-ray diffraction. Films deposited on GaSb(001) at substrate temperatures below 120 °C are amorphous in RHEED similar to Fig. 1 at 100 s, with a featureless diffraction pattern. Between 180 and 210 °C, we observe the epitaxial growth as shown in Figs. 1–3. Above 210 °C, notable desorption sets in with a decreasing growth rate of the film. At temperatures higher than 270 °C, the growth rate is 0. The growth window therefore is relatively narrow.

Using a high-power pulsed neodymium doped yttrium aluminum garnet laser, the epitaxial GST films can be amorphized and recrystallized again. As-grown, amorphized, and recrystallized locations were investigated by Raman spectroscopy. The corresponding spectra were recorded with a

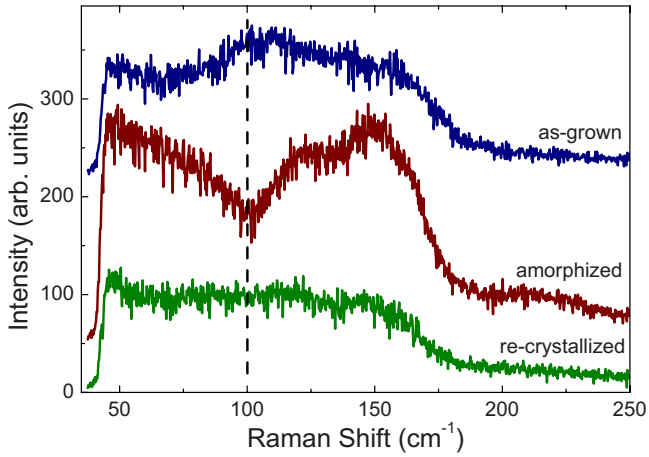

FIG. 4. (Color online) Room-temperature Raman spectra from a 65 nm thick epitaxial GST/GaSb(001) film for as-grown, amorphized, and recrystallized locations on the sample. The sharp cutoff near 40 cm^{-1} is due to the filter function of the Raman spectrometer.

triple spectrometer using the 676.1 nm line of a Kr^+ laser for excitation and a microscope objective for excitation and detection. The power density on the sample was about 80 kW/cm^2, just below the value where we observed sample damage due to laser heating. The sample was placed in a vacuum chamber during the experiment in order to avoid Raman signals from air close to the sample surface.

In Fig. 4, we compare the Raman spectra of the vibrational modes from three different positions on the same GST sample. The first spectrum represents the as-grown epitaxial material. For the second spectrum, the GST film has been amorphized by a single intense laser pulse with a pulse duration of 60 ps. Recrystallization is performed using about 400 laser pulses at 20 Hz repetition rate and half the switching pulse intensity, resulting in a structure that produces the third spectrum. The Raman spectrum obtained from as-grown material reveals a rather broad band between 80 and 180 cm^{-1} with the strongest intensity at 100 cm^{-1}. In contrast, the spectrum of amorphized material shows a clear maximum at 150 cm^{-1}. This spectral change closely resembles the transition from the crystalline to the amorphous state of sputtered GST.[3] In accordance with the model presented in Ref. 3, the shift of the Raman peak to higher wavenumbers reflects the shorter and stronger bonds in the amorphous phase. The increase in the Raman intensity toward 50 cm^{-1} is attributed to the Bose peak, which is characteristic for amorphous solids.[11,12] The larger integrated Raman signal from amorphized material can be attributed to the reduced reflection of the incident laser light and the increased probing depth caused by the reduced optical absorption in amorphized GST.[13] Finally, the Raman spectrum from recrystallized material is again similar to the one from as-grown material. However, the clear maximum at 100 cm^{-1} is now missing, which indicates that the recrystallization procedure is unable to fully recover the structure of the as-grown GST film.

In conclusion, we have fabricated and characterized epitaxial GST/GaSb(001) films using MBE. X-ray and RHEED measurements confirm the fcc structure of the films; x-ray fluorescence confirms their composition. Streaks along ⟨111⟩ in reciprocal space indicate that the Peierls distortion observed by EXAFS is preferentially oriented along ⟨111⟩ directions and hence resolve the apparent inconsistency between powder diffraction and EXAFS results. Raman scattering experiments reveal a signature corresponding to GST in the as-grown and laser-switched states. We expect that such epitaxial films will allow more detailed investigations of the structural changes during switching as the GST grows predominantly in the cube-on-cube orientation.

The authors would like to acknowledge the support of Steffen Behnke, Claudia Herrmann, and Anne-Kathrin Bluhm. Support for this work was provided by the Deutsche Forschungsgemeinschaft (BR 1723/3–1) and the Japan Science and Technology Agency through an international research corporation grant.

[1] M. Wuttig, Nature Mater. **4**, 265 (2005).
[2] N. Yamada and T. Matsunaga, J. Appl. Phys. **88**, 7020 (2000).
[3] A. V. Kolobov, P. Fons, A. I. Frenkel, A. L. Ankudinov, J. Tominaga, and T. Uruga, Nature Mater. **3**, 703 (2004).
[4] B. Jenichen, W. Braun, V. M. Kaganer, A. G. Shtukenberg, L. Däweritz, C.-G. Schulz, and K. H. Ploog, Rev. Sci. Instrum. **74**, 1267 (2003).
[5] B. Z. Nosho, B. R. Bennet, E. H. Aifer, and M. Goldenberg, J. Cryst. Growth **236**, 155 (2002).
[6] F. Maeda, M. Sugiyama, and Y. Watanabe, Phys. Rev. B **62**, 1615 (2000).
[7] W. Braun, H. MÃller, and Y.-H. Zhang, J. Vac. Sci. Technol. B **16**, 1507 (1998).
[8] T. Matsunaga and N. Yamada, Jpn. J. Appl. Phys., Part 1 **41**, 1674 (2002).
[9] T. Matsunaga, N. Yamada, and Y. Kubota, Acta Crystallogr., Sect. B: Struct. Sci. **60**, 685 (2004).
[10] T. Matsunaga and N. Yamada, Phys. Rev. B **69**, 104111 (2004).
[11] K. S. Andrikopoulos, S. N. Yannopoulos, A. V. Kolobov, P. Fons, and J. Tominaga, J. Phys. Chem. Solids **68**, 1074 (2007).
[12] K. A. Blanks, J. Phys. Chem. Solids **59**, 1279 (1998).
[13] B. S. Lee, J. R. Abelson, S. G. Bishop, D. H. Kang, B. K. Cheong, and K. B. Kim, J. Appl. Phys. **97**, 093509 (2005).